Optimization of biomass pyrolysis vapor upgrading using a laminar entrained-flow reactor system

Braden Peterson,[a,] Chaiwat Engtrakul,[b] Tabitha J. Evans,[a] Kristiina Iisa,[a] Michael J. Watson,[c] Mark W. Jarvis,[a] David J. Robichaud,[a] Calvin Mukarakate,[a] and Mark R. Nimlos[a]*

[a]National Bioenergy Center, National Renewable Energy Laboratory, 15013 Denver West Parkway, Golden, CO 80401-3393, USA. E-mail: braden.peterson@nrel.gov

[b]Chemistry and Nanoscience Center, National Renewable Energy Laboratory, 15013 Denver West Parkway, Golden, CO 80401-3393, USA.

[c]Johnson Matthey Technology Centre, PO Box1, Belasis Avenue, Billingham, Cleveland TS23 1LB, UK

KEYWORDS. Catalytic fast-pyrolysis, HZSM-5, biomass, laminar entrained-flow reactor

ABSTRACT. A bench-scale continuous-flow catalytic fast-pyrolysis (CFP) reactor system was implemented for the optimization of CFP and screening of catalysts to gain insight into commercial scale CFP processes across various reactor types. Operated in an *ex situ* configuration, tandem laminar entrained-flow pyrolyzer and vapor-phase upgrading reactors were optimized to successfully demonstrate CFP of pine over two different zeolite catalysts. Mixing-enhancers within the vapor-phase upgrader induced laminar flow dynamics with larger Reynold's numbers, thus enhancing heat and mass transfer and in turn CFP conversion. Real-time analysis of products was accomplished via molecular beam mass spectrometry (MBMS),

while light gas yield was determined using non-dispersive infrared (NDIR) analysis. The transfer of the pyrolysis vapors to the vapor-phase upgrader was investigated to gain insight into optimal transfer-line conditions for limiting secondary thermal cracking and preserving carbon in the *ex situ* CFP process. The products were comparable to those previously obtained from fixed bed and fluidized bed reactor systems as well as entrained-flow riser reactor systems. Similar trends in catalyst deactivation were observed for the laminar entrained-flow reactor system with decreasing catalyst-to-biomass ratio as reported in the literature. Under optimized continuous-flow conditions, constant catalyst activity was maintained, suggesting that the laminar entrained-flow reactor system was a viable option for the CFP of pine. Minor differences in catalytic activity were observed for the two catalysts tested.

Introduction

Catalytic fast-pyrolysis (CFP) of biomass has the potential to produce valuable fuel intermediates for the production of renewable transportation fuels.[1-15] During fast-pyrolysis, 70-75 wt%[16-19] of the biomass can be converted into oxygenated vapor products, including various alcohol, acid, carbonyl, methoxy phenol, and anhydrosugar compounds.[20,21] Upgrading of the oxygenated vapors by catalytic deoxygenation in CFP is necessary to remove chemically bound oxygen to improve the quality of the fast-pyrolysis product.[1,2,4-7,22] One of the main challenges associated with CFP is catalyst deactivation. Currently, solid acid catalysts such as zeolites are commonly used for the CFP of biomass. The acidity of these materials promotes pyrolysis vapor deoxygenation through dehydration, decarboxylation, decarbonylation, and catalytic cracking reactions. In addition, some acid zeolites, such as HZSM-5, promote chemical condensation, oligomerization, isomerization, alkylation, cyclization, and aromatization reactions via phenolic pool and hydrocarbon pool mechanisms.[23-26] Acidic zeolite catalysts have a high tendency to

deactivate due to the formation of coke and must be continuously regenerated.[3,11,27-33] Various reactor configurations, including fixed bed, fluidized bed, and entrained-flow systems have been utilized to study CFP in combination with regeneration methods to remove the coke from the catalyst as CO and CO_2 via oxidative treatment.[34-36] A range of mechanisms exists for understanding the formation of coke in zeolites. Several investigations have concluded that coking occurs due to the formation of coke precursors, such as alkylated aromatic hydrocarbons and polycyclic aromatic hydrocarbons, near catalyst pore openings. An increase in these coke precursors leads to more surface coke that eventually blocks access to the pores, thus deactivating the catalyst.[11,27,28,30-33] Recently, Fan *et al.*[28] and Shao *et al.*[31] demonstrated that the contact time between the pyrolysis vapors and the catalyst must be minimized so that the resulting deoxygenated CFP products can be desorbed before reacting further to form polycyclic aromatics (i.e., coke precursors). In addition, flow-rates including the ratios of pyrolysis vapors, carrier gases, and catalysts are operational parameters that are critical for controlling the catalyst and vapor residence times and limiting the contact time between the catalyst and pyrolysis vapors.[37-39] The influence of these operational parameters and overall reactor design on CFP carbon efficiency must be investigated to gain a thorough understanding of the potential for implementing CFP at industrially relevant scales.

It has been shown previously that small-scale reactor studies are essential to understand the influence of operating parameters and reactor design on the extent of the catalytic reactions and quality of the products. Both micro- and bench-scale reactor systems with fixed and fluidized beds, respectively, were successfully utilized for the *ex situ* CFP of yellow pine over HZSM-5.[26,40-45] These studies showed a correlation between product selectivities and the degree of catalyst deactivation, which was in turn dependent on the catalyst-to-biomass ratio used for the

conversion process. Specifically, the CFP oil oxygen content and oil yield were determined to be negatively correlated to the catalyst-to-biomass ratio for both fixed bed and fluidized bed systems. At high catalyst-to-biomass ratios, fully deoxygenated aromatic hydrocarbons (e.g., benzene, toluene, xylenes, and naphthalenes) were produced while at low catalyst-to-biomass ratios, the catalyst was deactivated and the vapor product was similar in composition to pure pyrolysis vapors (e.g., levoglucosan, carboxylic acids, furfurals, guaiacol and substituted guaiacol derivatives). Intermediate catalyst-to-biomass ratios produced partially deoxygenated CFP products such as furans, phenols, and cresols. Entrained-flow reactors (e.g., circulating fluidized bed reactors) have been successfully implemented in CFP processes.[34,46-48] In contrast to fixed bed and fluidized bed operations, entrained-flow systems allow for constant catalyst activity to be maintained by employing a single-pass, fast-contacting mode for the catalyst and pyrolysis vapors. Here, pyrolysis vapors contact the catalyst during a single pass through the reactor prior to vapor-catalyst disengagement where the contact time is limited to less than two seconds.[46-49] Iliopoulou *et al*.[49] conducted *in situ* CFP experiments where biomass was directly added to an entrained-flow riser reactor containing either HZSM-5 or metal-modified HZSM-5 catalysts. The results of their experiments showed significant improvement in the yields compared to previous experiments in which the catalyst was contained in a fixed bed or fluidized bed operating in both *in situ* and *ex situ* CFP modes. Typically, the catalyst-to-biomass ratios in these experiments were significantly greater than 1, which resulted in products with low oxygen content. Comparatively, CFP oil oxygen contents were lower in these entrained-flow experiments with similar yields compared to fixed bed experiments, implying higher carbon efficiencies in entrained-flow systems.[49]

As the need for assessing the commercial viability of bio-fuels becomes more prominent, it is important to characterize the CFP process efficiency associated with scale-up using various reactor types, so that efficient conversion of biomass to fuels can be realized at the commercial scale. To this end, a custom bench-scale tandem laminar entrained-flow reactor (LEFR) system was designed, built, and implemented for the optimization of CFP and screening of catalysts to gain insight into commercial scale CFP processes across various reactor types. This novel reactor system was compared to previously used fixed bed and fluidized bed reactor systems as well as entrained-flow riser reactor systems for the *ex situ* CFP of biomass over zeolite-based catalyst materials. Two different HZSM-5 zeolite catalysts were used to demonstrate the novel reactor system's value as a tool for investigating the operating parameters for the catalytic conversion of biomass. The two solid acid catalysts were selected on the basis of their deoxygenating activities resulting from acid-catalyzed reactions, including phenolic and hydrocarbon pool chemistries. Our studies verified that the LEFR system was a viable bench-scale CFP reactor for the upgrading of biomass. Catalyst deactivation was successfully monitored and indicated that this platform was a useful screening tool to assess catalyst activity. The pyrolysis reactor and transfer-line conditions between the tandem laminar entrained-flow reactors were controlled to maintain a high viable pyrolysis vapor yield in the *ex situ* CFP process. An optimal balance between transfer-line residence time and temperature was achieved to limit secondary thermal cracking of pyrolysis vapor.[50,51] Thermal cracking leads to carbon losses in the form of CO, CO_2, and light hydrocarbons.[20,50,52-54] Carbon loss to light gases results in reduced viable pyrolysis vapor yields, thereby negatively impacting CFP efficiencies. The vapor-phase upgrading reactor was operated at various temperatures to determine optimal conversion in conjunction with the pyrolysis vapor yield to achieve optimal CFP product composition and overall yield.

Experimental Materials and Methods

Entrained-flow Reactor System Overview

A general schematic diagram for the LEFR system is shown in Figure 1 while a more detailed process flow diagram is shown in Figure S1 of the Supporting Information. The employed backpressure-controlled CFP LEFR system was comprised of two tandem vertical stainless steel tubular reactors heated via resistive heater systems joined by heat-traced transfer-lines and a char cyclone/hot-gas filtration setup. In the first LEFR, functioning as a pyrolyzer, biomass was fed into the top of the reactor and entrained in nitrogen (N_2) carrier gas in a downward-flow fashion. Pyrolysis vapors produced in this first reactor were transferred through a heated transfer-line to a char cyclone to remove char fines before moving through a hot-gas filter (HGF). The filtered vapors were subsequently transferred to the side inlet of the second LEFR, functioning as a vapor-phase upgrading (VPU) reactor, and contacted with the catalyst to facilitate upgrading. The resultant heat-traced effluent was sent to a cyclone to disengage solids and filtered to remove remaining catalyst fines. During optimization and catalyst screening experiments (described below), a slipstream of the filtered vapors was analyzed, in real-time, via molecular beam mass spectrometry (MBMS, Extrel Core Mass Spectrometers). The MBMS product slipstream undergoes adiabatic expansion through a 250 μm orifice into a vacuum chamber held at ~100 mtorr, which rapidly cools the product stream, effectively freezing the chemistry and hindering further reactions. The resulting cooled product gas is then skimmed into a molecular beam to be positively ionized prior to being mass-resolved and analyzed via a quadrupole mass spectrometer. As MBMS separates and identifies compounds based on mass (m/z) and because the employed system has a resolution of 0.1 amu, full speciation was not achieved, leaving isomers unresolved. Speciation of pyrolysis and CFP products has been completed on similar

systems in previous studies with results from these studies used in this work.[20,21,26] The remaining effluent was directed into a gas conditioning system to actively and thermally condense product vapors via an electrostatic precipitator (ESP) and cooled thermal condenser, respectively. Condensable vapors were sequentially separated into organic and aqueous phases within the gas conditioning system. A coalescing filter at the outlet of the conditioning system trapped any fugitive vapors. The resulting conditioned product stream was sampled via a gas bag slipstream, to be analyzed offline by GC-MS, while light gases, CO, CO_2, and CH_4, were analyzed online via non-dispersive infrared (NDIR, CAI ZRE Gas Analyzer, Type: ZRECBT31-JMJMH-LYYC2CE-YYYAA) analysis. System control was achieved through an Opto22 programmable automated control package (PAC, Project Professional Version 9.3) using a human machine interface (HMI). Total system pressure was controlled in the pyrolyzer reactor by a feedback-controlled backpressure regulator located at the system outlet. Therefore, pressure downstream of the pyrolyzer was dependent upon system flow dynamics. Additional details regarding control configuration, including operational and temperature control configurations, are given in the Supporting Information (Section 1). Of note, the pyrolyzer LEFR is controlled primarily by gas temperature while the VPU LEFR and transfer-lines were controlled by wall temperature.

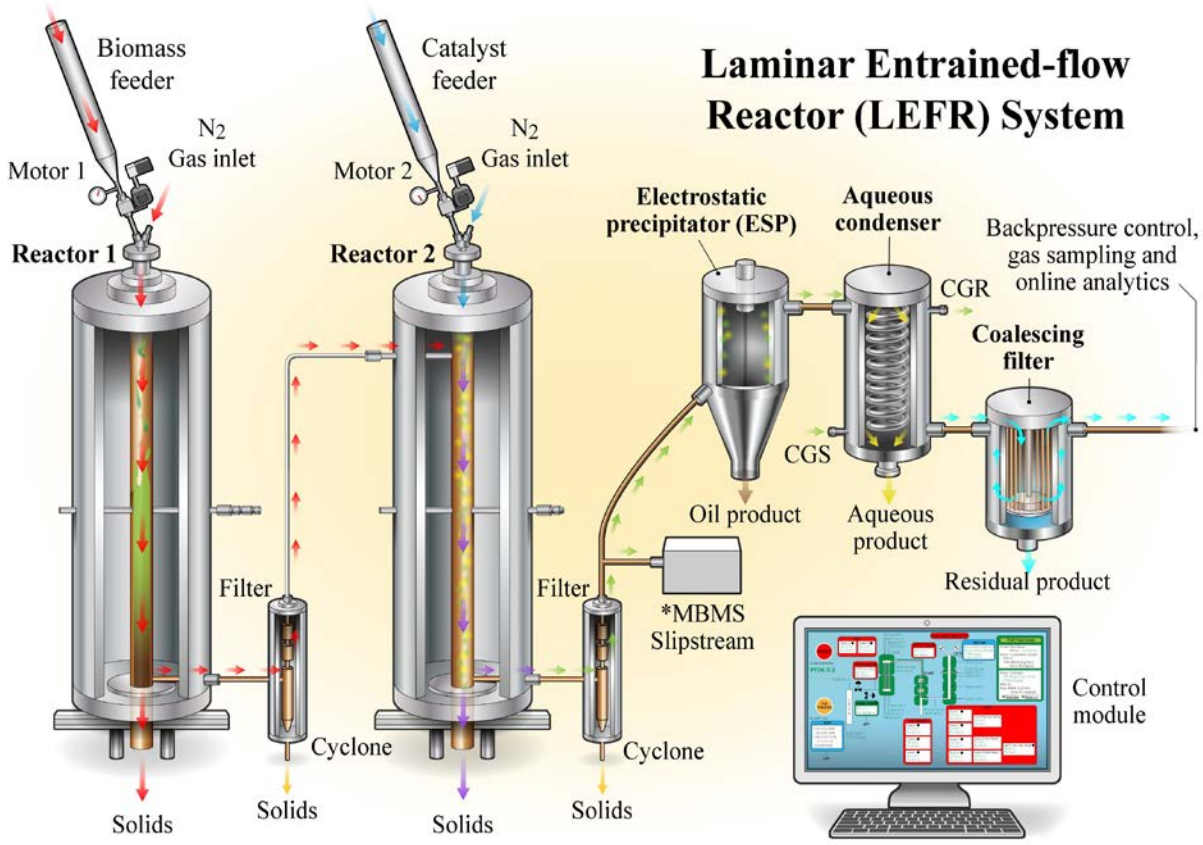

Figure 1. Laminar entrained-flow reactor (LEFR) system showing the pyrolyzer (Reactor 1), char cyclone + hot-gas filter, vapor-phase upgrader (VPU, Reactor 2), catalyst cyclone + catalyst filter, electrostatic precipitator (ESP), aqueous condenser, and coalescing filter along with slipstream analytics (molecular beam mass spectrometer (MBMS) and gas bag sampling) and online analysis (non-dispersive infrared (NDIR) analyzer). Aqueous condenser is a counter-flow heat exchanger (thermal condenser) with the associated chilled glycol supply (CGS) and chilled glycol return (CGR) shown. *MBMS utilized a slipstream via a flow-by plate and was solely implemented during optimization and screening studies.

Biomass and Catalyst Materials

Southern yellow pine was used as biomass feedstock throughout all experiments and was supplied by Idaho National Laboratory (INL). Prior to being used, the pine was mechanically reduced in size via knife-milling followed by sieving to a 60-80 mesh (250-125 μm) particle size distribution. The composition of yellow pine was 42 wt% cellulose, 21 wt% hemicellulose and 30 wt% lignin.[26] Elemental analysis was accomplished with a LECO TruSpec CHN module, showing elemental composition on a wet basis of 49.6 wt% C, 6.3 wt% H, 43.5 wt% O, < 0.1 wt% N, 0.1 wt% S, and 0.4 wt% ash, and a water content of 2.9 wt%.[40,55] Two catalyst materials were investigated; Grace Davison (GD) HZSM-5 and Johnson Matthey (JM) HZSM-5 catalysts. The Grace Davison and Johnson Matthey catalysts were both bound, spray-dried materials with a nominal particle size of 70 μm containing approximately 50 wt% HZSM-5. Both these materials possessed free-flowing rheological properties due to their spray-dried spherical particle morphologies, which allowed for trouble-free continuous catalyst feeding. While the balancing component of these spray-dried catalysts was comprised of binder materials and other additives, complete compositional specifications were not available from the commercial suppliers. The catalytic activity of these two materials is largely associated with the acid sites of the zeolites, which was the basis for their selection and testing in the LEFR system. Prior to use, all catalysts were calcined in a muffle furnace using the same procedure; ramp to 550°C at 3°C/min, hold for 4 h and allow to passively cool to ambient temperature.

Transfer-line Temperature Optimization and Reactor Optimization

Thermal cracking of pyrolysis vapors is dependent upon temperature and residence time. As the total residence time within all transfer-lines was below 1 s, thermal cracking minimization

focused on optimizing transfer-line temperature. Therefore, to investigate the temperature dependence of thermal cracking of pyrolysis vapors in the employed system, a series of experiments were conducted with the system downstream of the pyrolyzer LEFR, including the VPU LEFR (without the use of catalyst), functioning as a transfer-line (inclusion of the VPU as a transfer-line during optimization ensures further minimization of thermal cracking during CFP experiments). These entailed pyrolyzing biomass at 500°C (10 g/h feedrate) and sweeping the transfer-line temperature from 375-475°C, in 25°C increments, while monitoring product changes via MBMS and measuring the quantity of light gases as CO, CO_2, and CH_4 via NDIR. Since these light gases are partially produced by thermal cracking of pyrolysis vapors,[20,50,52-54] the quantity of gases produced should be proportional to transfer-line temperature.

Optimization of the pyrolysis reactor entailed sweeping the reactor gas temperature from 400-600°C in 25°C increments while measuring light gas and char yields. As light gas and char production are negatively interdependent on temperature,[53,56] the intersection of light gas and char yield curves as a function of temperature gives the optimal temperature at which pyrolysis vapor production is maximized. Initial VPU reactor optimization entailed mass and heat transfer enhancement through employment of coaxial mixing-enhancers as documented in the Supporting Information. The employed mixing-enhancers are shown in Figure S2. Further VPU reactor optimization entailed conducting upgrading experiments at a fixed pyrolysis vapor composition (~0.04 g biomass/g N_2) while sweeping the reactor wall temperature from 400-625°C to determine where optimal upgrading occurred. Optimal upgrading was gauged by the maximization of m/z signals for benzene (m/z =78), toluene (m/z = 91), ethyl benzene (m/z =106), and xylenes (m/z =106) (BTEX) with simultaneous minimization of the CO_2 signal (m/z = 44) via MBMS analysis at the catalyst-to-biomass ratio of 10. A catalyst-to-biomass ratio of 10

was chosen based on initial non-optimized screening results that showed partial deoxygenation of the pyrolysis vapors. The GD HZSM-5 catalyst was used throughout the VPU LEFR optimization experiments. The MBMS was solely used for monitoring the degree of upgrading during reactor optimization and catalyst screening experiments (described below) and not for the subsequent mass balance experiments.

System Validation: Screening Studies, Mass Balance Experiments, and Catalyst Deactivation

Experiments were conducted to investigate CFP performance as a function of catalyst and catalyst-to-biomass ratio in the LEFR system using real-time analysis of products via MBMS and NDIR. Prior to the performance evaluation experiments, system optimization studies resulted in the configuration outlined in both Figure 1 and Figure S1. A series of catalyst-to-biomass ratio experiments were conducted to both determine the optimal ratio for pyrolysis vapor upgrading to BTEX via CFP and to compare the performance of two selected HZSM-5-based catalysts. The purpose of comparing two catalysts was to demonstrate that the LEFR system can be used as a catalyst screening tool to evaluate catalytic performance. The catalyst-to-biomass ratio was swept by varying both biomass feedrate at constant catalyst feedrate and the catalyst feedrate at constant biomass feedrate. The biomass feedrate ranged from 5 g/h to 40 g/h while the catalyst feedrate spanned from 50 g/h to 475 g/h with combinations of these feedrates allowing the catalyst-to-biomass ratio to range between ~2-30. The various catalyst-to-biomass ratios evaluated for the two catalysts are provided in Table 1. The majority of the MBMS screening data associated with these catalyst-to-biomass ratio scoping studies were omitted for brevity, while the pertinent data showing acceptable performance is presented below (Figures 4 and 5).

Table 1. Evaluated catalyst-to-biomass ratios for two commercially available HZSM-5 catalysts: Grace Davison and Johnson Matthey.

Catalyst ID	Biomass Feedrate (g/h)	Catalyst Feedrate (g/h)	Catalyst-to-Biomass Ratio
Grace Davison HZSM-5	11.1	309.2	28
	11.7	103.0	9
	11.7	75.2	6
	23.8	475.1	20
	21.3	279.5	13
	23.8	255.7	11
	22.0	213.0	10
	23.8	117.4	5
	22.0	63.3	3
	22.5	59.0	3
	40.8	184.6	5
	40.7	72.1	2
Johnson Matthey HZSM-5	12.3	360.6	29
	12.3	359.4	29
	12.3	264.1	21
	12.3	155.6	13
	22.0	386.6	18
	22.0	290.8	13

Subsequent to the performance evaluation experiments using the MBMS, a replicate series of mass balance system validation experiments were conducted using the GD HZSM-5 catalyst at a catalyst-to-biomass ratio of ~25. The mass balance experimental data complemented the MBMS experimental data, where all reactor conditions were the same as those used in the performance evaluation experiments. The mass balance experiments employed a biomass feedrate of 10 g/h. Due to the high catalyst demand (~250 g/h) and the catalyst hopper volume limitations, these experiments were limited to 1 h time-on-stream (TOS). Gravimetric analysis was conducted on the char catch-pot, char cyclone, catalyst catch-pot, catalyst cyclone, ESP product, condenser product fractions, and coalescing filter for each replicate. Coked catalyst materials were analyzed via thermogravimetric analysis (TGA) to quantify the amount of coke deposited. Aliquots of these coked catalysts were washed with xylene and the washes were analyzed by GC-MS to identify any trapped hydrocarbons in the catalyst pore structure. Trapping of aromatic hydrocarbons within HZSM-5 catalyst materials has been shown to occur as a result of coking reactions.[28,29,57] Due to the short TOS, the majority of CFP product accumulated on the glass surface of the ESP (~1.0 g upgraded oil). Thus, the ESP product was solubilized in a fixed and known amount of acetone prior to being analyzed via GC-MS and gel permeation chromatography (GPC). Aqueous product fractions collected in the thermal condenser (downstream of the ESP) were analyzed by GC-MS and Karl Fischer (KF). The residual carbon build-up within the LEFR system during each experiment (system coke) was quantified by burning off the material under flowing air (200 SCCM in 3.4 SLM N_2) while monitoring CO, CO_2, and CH_4 evolution via NDIR. Details regarding data acquisition and analysis via MBMS, NDIR, GC-MS, TGA, GPC, and KF are provided in the Supporting Information (Section 2).

Results and Discussion

Transfer-line Temperature Optimization

The transfer-line secondary thermal cracking studies are summarized by data presented in Figure 2. Figure 2A shows the pyrolysis products via MBMS after being exposed to various transfer-line temperatures. The total light gas yield, including CO_2, was determined via NDIR analysis as a function of transfer-line temperature and increased with increasing transfer-line temperature (Figure 2B). These results are in agreement with previous pyrolysis vapor thermal cracking studies.[50,52,54] Furthermore, as shown in Figure 2A, higher molecular weight species ($m/z > 180$) were more prevalent at higher temperatures (e.g., 475°C). Chemical condensation of lower molecular weight compounds is suggested to be responsible for the prevalence of higher molecular weight species at the higher temperatures. Surprisingly, a slight increase in higher molecular weight species at 375°C was observed. We suggest that physical vapor condensation was beginning to occur at 375°C leading to clustering within the MBMS sampling system and thus, the increase in concentration of higher molecular weight species. Additional thermal cracking experiments below 375°C resulted in significant transfer-line clogging due to physical vapor condensation. Since the light gas yields (NDIR) increased above 400°C and vapor condensation commenced at 375°C, the optimal transfer-line temperature was chosen to be 400°C and therefore utilized moving forward.

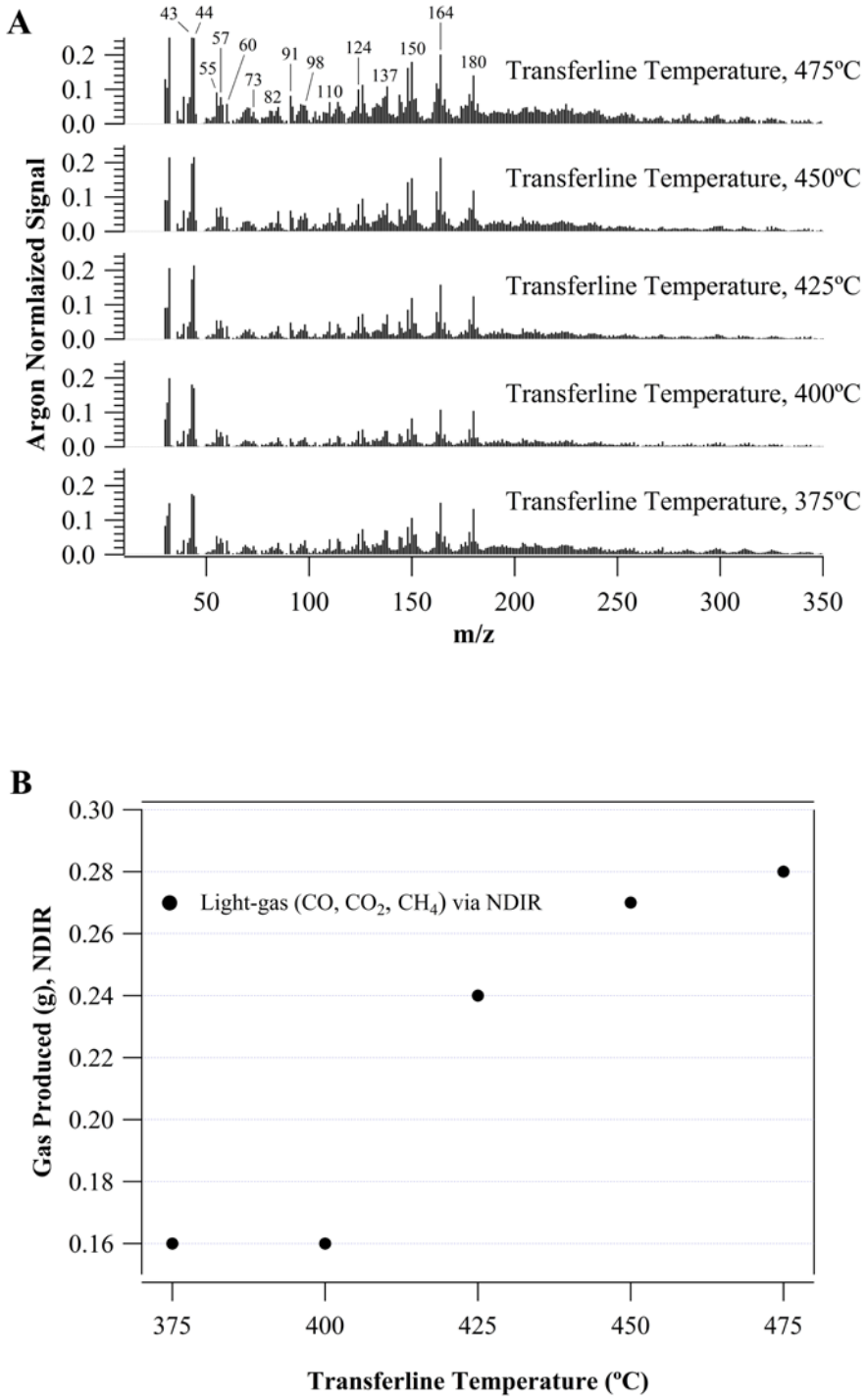

Figure 2. A) Mass spectra via MBMS for thermal cracking of pyrolysis vapors from 375-475°C. B) Light gas (CO, CO_2, CH_4) production during thermal cracking studies as determined via NDIR.

Pyrolyzer LEFR Optimization

The ideal pyrolysis LEFR temperature was determined by measuring the biomass char and light gas yields as a function of reactor gas temperature. As shown in Figure 3, the optimal temperature for pine pyrolysis was approximately 480°C (gas temperature) based on the intersection of the two curves for biomass char and light gas production, where each was at a minimum. The total of these two values is also plotted in Figure 3, where the difference between their sum and 100% gives the theoretical pyrolysis vapor yield. Maximum theoretical pyrolysis vapor yield is shown to occur when the sum of char and light gas yields is minimized. Based on previous work by Thompson *et al.*, which correlated the degree of pyrolysis with char coloration, pyrolysis in the LEFR system at the minimization point (480°C) was determined to be incomplete since the LEFR-produced char was mainly brown in color.[58] Additionally, incomplete pyrolysis was clearly observed at temperatures below 480°C and further supported by the elevated char yields obtained in the LEFR system relative to other CFP systems. Based on previous work,[29,41-43,56,59,60] the pyrolyzer was operated at a gas temperature of 500°C (marginally above 480°C) for the pine pyrolysis. It should be noted that the optimal pyrolysis reactor temperature is dependent on the biomass feedstock.

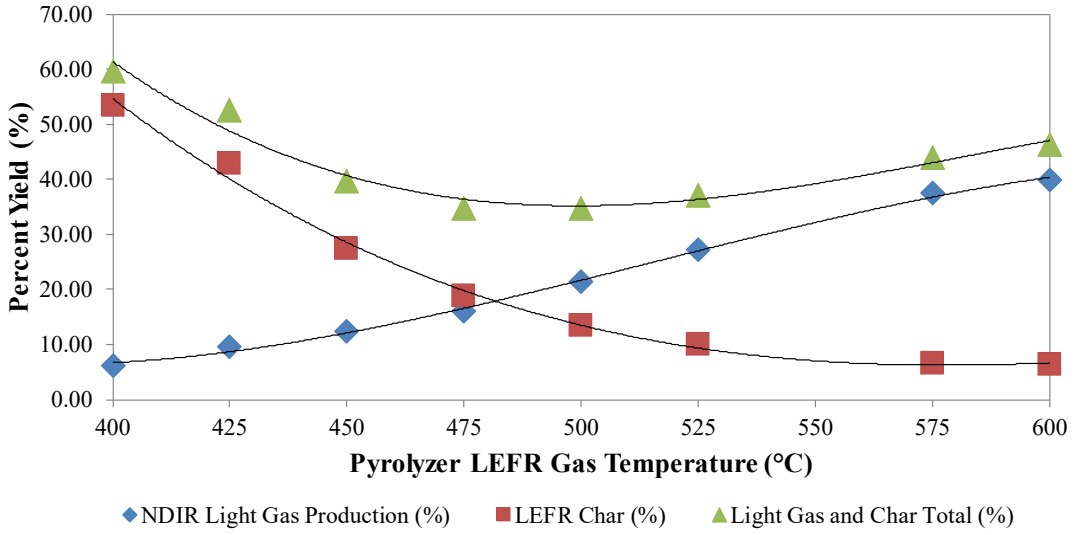

Figure 3. Pyrolyzer laminar entrained-flow reactor (LEFR) char and light gas yield as a function of reactor gas temperature with associated best-fit trendlines. Co-minimization of char and light gas yields as a function of temperature gives the optimal temperature for maximum theoretical pyrolysis vapor production, shown here to be a value of ~480°C. Maximum theoretical pyrolysis vapor yield is 100% minus the sum of char and light gas yields.

VPU LEFR Optimization

Utilizing the reactor optimization procedure described in the Experimental Methods and Materials section, the optimal temperature for the VPU LEFR was determined to be 475°C (reactor wall temperature). Significant pyrolysis vapor upgrading (deoxygenation) was observed at a catalyst-to-biomass ratio of 10. At this ratio, BTEX hydrocarbons were observed in addition to pine pyrolysis components (primary vapor products). Based on the catalyst-to-biomass ratio sweep experiments (see Experimental Methods and Materials), optimal CFP for the LEFR

system occurred within the catalyst-to-biomass ratio range of 20-30. Under this condition, two catalyst materials were screened and compared (Figure 4). The MBMS spectrum in Figure 4A shows the characteristic pine pyrolysis peaks (primary vapor products: m/z 110, 124, 137, 138, 150, 164 and 180) expected for pure pyrolysis at 500°C.[20,21,26,40] Figure 4B shows the MBMS spectrum for CFP at a low catalyst-to-biomass ratio of 2 using a GD HZSM-5 catalyst. For this ratio there was a minor reduction in primary pyrolysis vapors and minimal upgrading to fully deoxygenated products based on the low production of BTEX (m/z 78, 91, 106). A significant BTEX enhancement and reduction of primary vapors was observed with a JM HZSM-5 catalyst using a catalyst-to-biomass ratio of 29 (Figure 4C). An improved CFP performance, based on BTEX enhancement and reduction of primary vapors, was observed for the GD HZSM-5 catalyst using a catalyst-to-biomass ratio of 28 (Figure 4D). Only minor conversion differences were observed between the JM HZSM-5 and GD HZSM-5 catalyst materials. To achieve results comparable to those obtained by Iliopoulou *et al.*,[49] the LEFR system was operated in a higher catalyst-to-biomass ratio regime (catalyst-to-biomass ratio > 25) when conducting mass balance experiments.

The TOS plot for the better performing catalyst (GD-HZSM-5; catalyst-to-biomass ratio = 28) is shown in Figure 5, where one-ring deoxygenated aromatic (m/z = 78, 91, 106), deoxygenated polyaromatic (m/z = 128, 142, 156), furanic (m/z = 82, 96, 98), phenolic (m/z = 94, 108, 122), and primary vapor (m/z = 124, 138, 150, 164, 180) products were trended as a function of time. As biomass was added to the reactor and pyrolyzed (Figure 5, see Biomass Feed Start at three minutes TOS), the concentration of all five groups of products increased. In contrast, upon catalyst feed initiation (Figure 5, see Catalyst Feed Start at eight minutes TOS), one-ring aromatics increased, while primary vapors, furans, and phenols decreased. These product trends

were expected for CFP where the conversion of primary vapors, furans, and phenols into BTEX was the favored process. The signal intensity for the polyaromatic species remained constant throughout pyrolysis and CFP (catalyst addition). Since deoxygenated polyaromatic species are not produced in pyrolysis, the constant signal intensity is believed to result from the fragmentation of lignin species during MBMS sampling to fragments with m/z values coinciding with 128, 142, and 156. This same phenomenon is believed to account for the signal intensity for one-ring deoxygenated aromatic species after biomass addition and prior to catalyst introduction. Deoxygenated polyaromatics are typically produced during CFP.[4,41-43,49] An increase in the signal intensity for deoxygenated polyaromatics upon catalyst addition (CFP) was not observed in Figure 5. Since the tuning of the MBMS was towards lower molecular weight species, the sensitivity required to detect any changes in the production of higher molecular weight species may have been limited. The absence or presence of higher molecular weight deoxygenated polyaromatics was verified by GC-MS. Here, these data confirmed that deoxygenated polyaromatics were absent in the pyrolysis oil product and present in the upgraded oil product. Upon ceasing biomass and catalyst feeds (Figure 5, see Feed Stop at eighteen minutes TOS), minor transient changes in CFP product composition were initially observed before product signals decreased to zero.

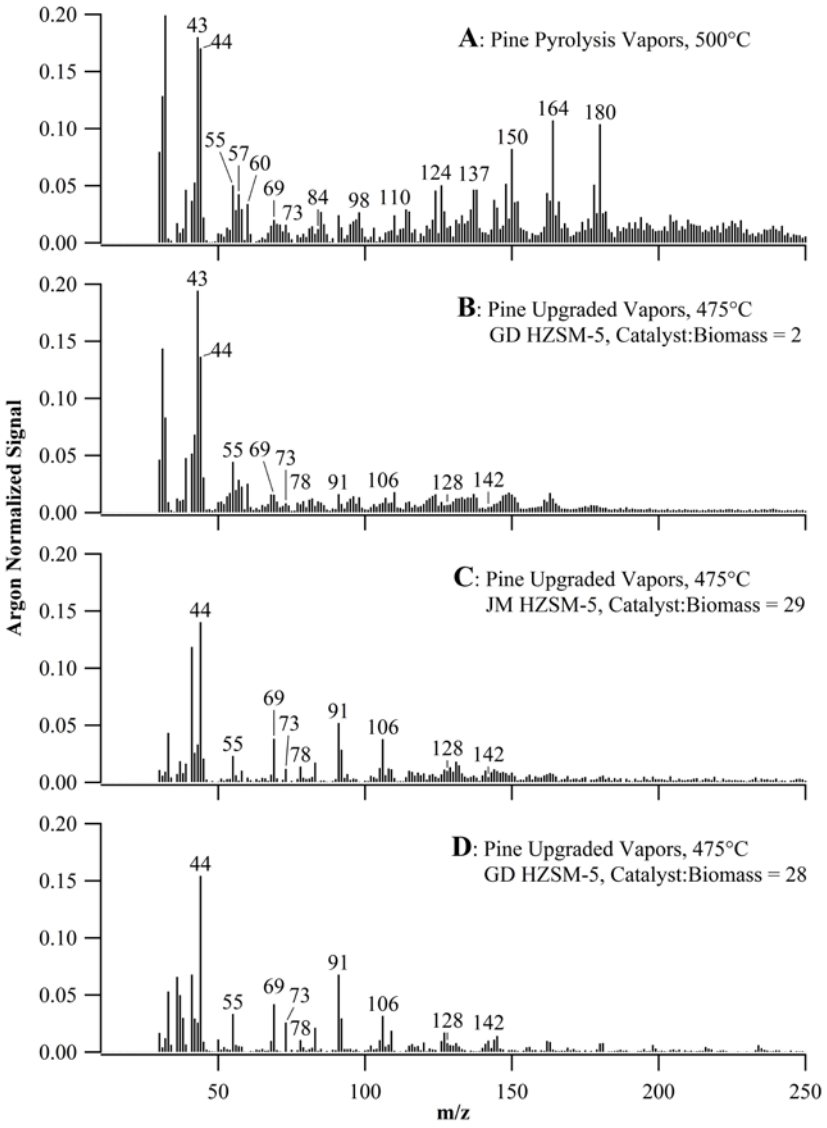

Figure 4. Mass spectra of (A) pure pyrolysis of pine at 500°C, (B) upgraded vapors using Grace Davison HZSM-5 (GD HZSM-5) at catalyst-to-biomass ratio = 2, (C) upgraded vapors using Johnson Matthey HZSM-5 (JM HZSM-5) at catalyst-to-biomass ratio = 29 and (D) upgraded vapors using GD HZSM-5 at catalyst-to-biomass ratio = 28. All upgrading experiments were conducted at 475°C wall temperature with pyrolysis at 500°C (gas temperature) and transfer-lines held at 400°C (wall temperature).

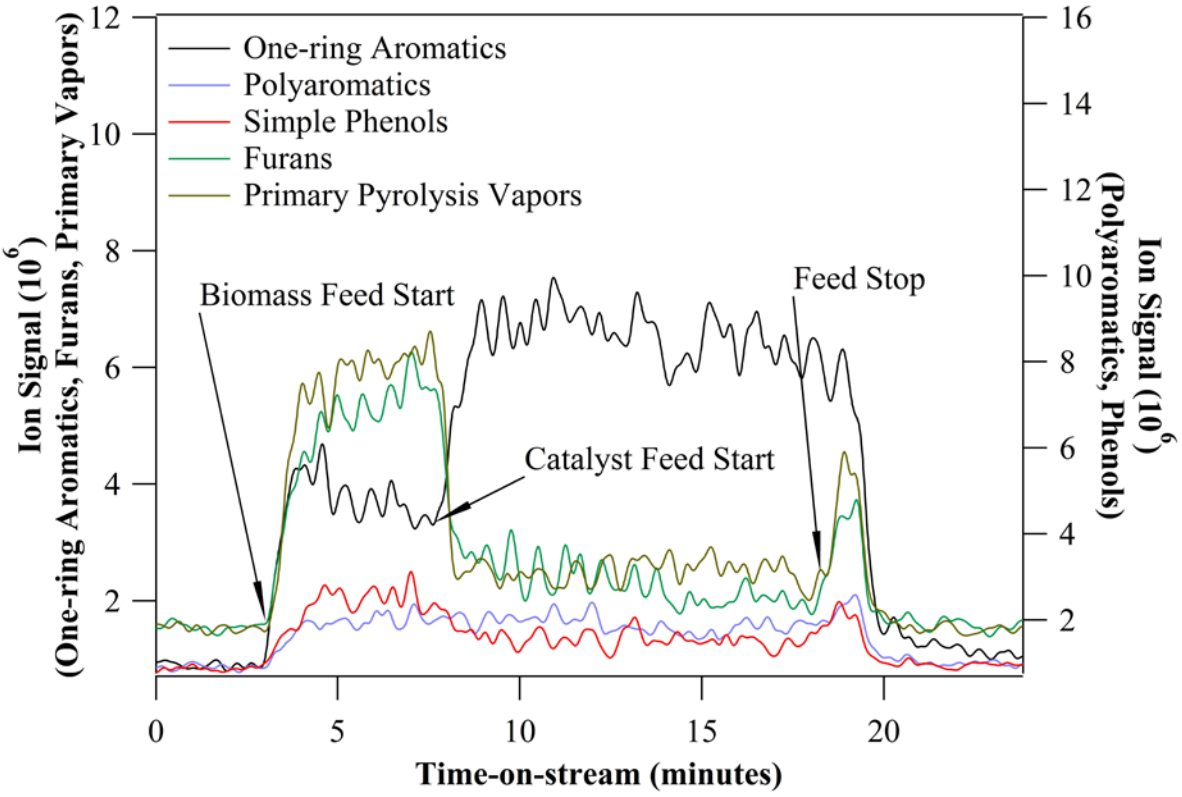

Figure 5. Time-on-stream plot showing initial pyrolysis at 500°C (gas temperature) and subsequent upgrading at 475°C (wall temperature) using Grace Davison HZSM-5 (GD HZSM-5) at a catalyst-to-biomass ratio of 28. Primary vapors decreased as upgraded products increased upon catalyst addition. The typical pyrolysis CFP product distributions were determined by MBMS and shown in Figure 4.

LEFR System Validation

CFP Mass Balance Comparison. Mass balance experiments yielded consistent data across three replicates as shown in Table 2. The CFP aqueous product yield (~27 wt%) was comparable to those obtained from other CFP reactor systems.[6,42,43,47,49] The char yields for the LEFR system

(~26 wt%) were higher relative to previous CFP of pine performed in a fixed bed reactor (8-12 wt%),[26,61] fluidized bed reactor (9-10 wt%),[42,43] and entrained-flow riser reactor (char + coke, 18 wt%).[49] As stated previously, the elevated char yield and brown-hued coloration can be attributed to incomplete pyrolysis in the pyrolyzer. This may be due to heat-transfer limitations as a result of the laminar flow dynamics in the pyrolyzer LEFR. Under these laminar flow conditions, heat transfer enhancement via radial fluid mixing is non-existent while less efficient convection of heat from the reactor walls to the reactive fluid is the primary mode of transport.[62] Because of this heat transfer limitation, the average biomass residence time in the isothermal pyrolyzer heat zone of ~6.5 s may be too short, further contributing to incomplete pyrolysis. It should be noted that residence times less than 6.5 s have been successfully utilized for pine flash-pyrolysis reactors employing turbulent flow dynamics.[17,18,39] Dimensional reactor changes to increase residence times within the pyrolyzer and/or turbulence within the reactor or a higher pyrolysis temperature may allow for more complete pyrolysis (optimization).

The light gas yield from the LEFR system (~22 wt%) was lower than previous CFP reports, which ranged from 30-34 wt%.[41,42,49,63] Relative to the entrained-flow riser reactor used by Iliopoulou *et al.*[49], there was ~34% less CO, ~27% less CO_2, and ~26% less CH_4 produced in the LEFR system during CFP. Typically, longer biomass vapor residence times in pyrolysis reactors lead to higher light gas yields.[50,51,54] The average residence time for the vapors in the VPU LEFR (~3.6 s) was greater than the residence time reported by Iliopoulou *et al.* for their entrained-flow riser reactor (< 2 s).[49] The lower light gas yields in the LEFR system can be attributed to incomplete pyrolysis and/or less thermal cracking since a lower VPU LEFR temperature was utilized (wall temperature, 475°C) relative to the higher entrained-flow riser reactor temperature (gas temperature, 500°C).[6,47-49]

The upgraded oil yields were lower (~14 wt%) compared to the yields obtained on entrained-flow riser[6,47,49] and fixed bed[26,49] reactors but similar to yields obtained with fluidized bed reactors.[42,43] These lower yields were attributed to incomplete pyrolysis that led to high char values (as stated above) and thus, less viable pyrolysis vapors (biomass) available for upgrading. In addition, upgraded oil yields have been shown to be negatively correlated to the catalyst-to-biomass ratio; larger catalyst-to-biomass ratios typically give rise to higher degrees of deoxygenation (lower oxygen content) but lower upgraded oil yields.[42] This operational process parameter could account for the lower upgraded oil yield in the LEFR system. Although, this is not conclusive as some oxygenated species were present in upgraded oil product as described below. It should be noted that the catalyst-to-biomass ratio is represented differently in fixed and fluidized beds compared to entrained-flow systems. In fixed and fluidized bed systems, the catalyst-to-biomass ratio is determined as the ratio of a fixed amount of catalyst and the integrated pyrolysis vapor flow while in entrained-flow systems, it is determined as the ratio of the respective catalyst and biomass feedrates.

Table 2. Replicate mass balance experimental results for the Grace Davison HZSM-5 catalyst and a catalyst-to-biomass ratio of ~25.

Product Type		Replicate 1 (wt%)	Replicate 2 (wt%)	Replicate 3 (wt%)
Solid Product	LEFR Char	24.4	23.6	24.7
	Cyclone Char	1.1	3.2	1.5
	System Coke	1.8	1.3	1.4
	Catalyst Coke	N/A	9.5	11.6
	Subtotal	27.3	37.6	39.2
Liquid Product	Aqueous	30.0	23.7	26.3
	Oil	13.5	14.1	13.6
	Coalescing Filter	0.1	0.3	0.7
	Subtotal	43.6	38.1	40.6
Gaseous Product	CO	11.5	12.5	11.7
	CO_2	8.2	8.6	9.3
	CH_4	0.7	0.7	0.7
	Subtotal	20.4	21.8	21.7
	Mass Balance Closure (Total)	91.3	97.5	101.5

Analyses of the Upgraded Oil and Aqueous Products. Gel permeation chromatography was utilized to characterize the upgraded oil obtained from the ESP during the mass balance experiments. The average molecular weight of the oil was 420 Da. This value was significantly higher than previously reported values for CFP oil.[43] Since the upgraded oil products were collected under continuous-flow conditions and elevated temperatures (~60°C), light molecular weight products (e.g., benzene, toluene) were driven off and the remaining products within the ESP may have polymerized to higher molecular weight species due to the prolonged exposure to

heat. Gas bag analysis showed the presence of BTEX components along with acetaldehyde, furans, and cyclopentanones in the system effluent. Further analysis of the oil by GC-MS showed the presence of upgraded products as well as oxygenated intermediate and primary vapor species. GC-MS analysis of the oil product and the slipstream MBMS analysis used in the performance experiments were utilized to indirectly assess pyrolysis vapor deoxygenation. Complementary CHNO analysis would have been beneficial for directly assessing deoxygenation but was not possible due to the low upgraded oil yields obtained (~1.0 g). Per the dimensional analysis discussion in associated Supporting Information (Section 3), heat and mass transport limitations are present in the VPU LEFR, potentially allowing portions of pyrolysis vapors to pass through the reactor without contacting catalyst or completely being upgraded. Based on Karl Fischer titration the aqueous product was on average 98 wt% water. The water-soluble organic compounds in the aqueous fraction were identified by GC-MS. The compounds were grouped into acids (25.7 wt%), carbonyls (18.8 wt%), phenols (52.1 wt%), sugars (1.2 wt%), and ethers (2.2 wt%).

Coke Analysis. Thermogravimetric analysis of the coked catalyst materials indicated that the LEFR system produced higher total coke (system coke plus catalyst coke) yields compared to previous entrained-flow CFP studies. In the LEFR system, catalyst coke ranged from ~9-12 wt% while system coke spanned ~1.3-1.8 wt% (~10-14 wt% total coke). These values are similar to coke yields obtained in fluidized bed (~7-9 wt% as total coke)[42,43] and fixed bed (7-15 wt% as total coke)[26,40] systems but higher when compared to entrained-flow (~1-4 wt% as total coke)[47] systems. In all of the reactor systems, the majority of the coke resided on the catalyst. The preference for catalyst coke formation can be attributed to the large surface areas and acidic properties of the catalysts. Interestingly, fixed bed and fluidized bed coke yields have been

shown to be proportional to the catalyst-to-biomass ratio.[26,42,43] Therefore, the higher total coke yields in the LEFR system were reasonable due to the higher catalyst-to-biomass ratios employed. At higher catalyst-to-biomass ratios there is more catalyst surface area relative to biomass vapor. More accessible catalyst surface area allows for more vapor-catalyst interactions and subsequent acid-catalyzed reactions, both desired (deoxygenation reactions) and undesired (coking reactions). In addition, catalyst solvent extraction and supernatant characterization showed no evidence for the presence of polyaromatics (coke precursors) within the catalyst materials.

Conclusion

A novel tandem LEFR system was successfully designed, built, and implemented as a platform for CFP optimization and tool for catalyst screening to investigate CFP of pine biomass over HZSM-5. In this study, the system was optimized in terms of the pyrolyzer and VPU reactor temperatures, pyrolysis vapor transfer temperature, and the catalyst-to-biomass ratios required to achieve adequate upgrading in the VPU. Optimal pyrolysis and VPU temperatures were determined to be 500°C (gas temperature) and 475°C (wall temperature), respectively. It was shown as well that the optimal transfer-line wall temperature for pyrolysis vapors was 400°C (vapor residence time < 1 s), where a balance between physical and chemical condensation was established to minimize secondary thermal cracking of vapors. This preserved the quality of the pyrolysis vapors by minimizing carbon loss via light gases, CO, CO_2, and CH_4. Furthermore, it was demonstrated that, when using HZSM-5, catalyst-to-biomass ratios of ≥ 25 are required to achieve adequate upgrading of pyrolysis vapors in the LEFR system. The LEFR system was used to test and screen two commercially available HZSM-5 catalyst materials. A slight performance advantage was observed for the Grace Davison catalyst over the Johnson Matthey catalyst with

respect to BTEX production. Additional CFP optimization was achieved by enhancing vapor-catalyst mixing in the VPU. Although, heat and mass transfer limitations still existed due to laminar flow regimes within the reactor.

Post-optimization results were compared to results obtained previously from fixed bed and fluidized bed reactor systems as well as entrained-flow riser reactor systems.[26,34,40-49] Similar catalyst deactivation and CFP conversion trends as a function of catalyst-to-biomass ratio were observed in the LEFR system relative to other reactor platforms. The upgraded oil yields obtained from the LEFR system were lower compared to the entrained-flow riser reactor yields. These lower yields may be attributed to the high catalyst-to-biomass ratios employed in this study and/or incomplete pyrolysis. The advantage of the *ex situ* CFP in laminar entrained-flow mode was that constant catalyst activity could be maintained. This study validated the viability of the LEFR system as a CFP reactor platform with reasonable CFP mass closures and product selectivities when compared to fixed bed, fluidized bed, and entrained-flow riser reactor systems. Since the findings in this study apply to general reactor design, these findings can be used to give insight into commercial scale CFP process optimization across various established reactor types.

ASSOCIATED CONTENT

Supporting Information

Detailed overview of the laminar entrained-flow reactor (LEFR) system, data acquisition and analysis, and evaluation of employed vapor-phase upgrading (VPU) mixing-enhancers.

AUTHOR INFORMATION

Corresponding Author

*E-mail: braden.peterson@nrel.gov

Notes

The authors declare no competing financial interest.

ACKNOWLEDGMENT

This work was authored by Alliance for Sustainable Energy, LLC, the manager and operator of the National Renewable Energy Laboratory for the U.S. Department of Energy (DOE) under Contract No. DE-AC36-08GO28308. Funding provided by the U.S. Department of Energy's Office of Energy Efficiency and Renewable Energy (EERE) under Bioenergy Technologies Office (BETO). The views expressed in the article do not necessarily represent the views of the DOE or the U.S. Government. The U.S. Government retains and the publisher, by accepting the article for publication, acknowledges that the U.S. Government retains a nonexclusive, paid-up, irrevocable, worldwide license to publish or reproduce the published form of this work, or allow others to do so, for U.S. Government purposes. The authors would like to thank Kim Magrini, Yves Parent, Stuart Black, Steve Deutch, Kellene Orton, Anne Starace, and Anne Ware for analytical support and as well as for offering subject-matter expertise.

REFERNCES

(1) Asadieraghi, M.; Ashri Wan Daud, W. M.; Abbas, H. F. Heterogeneous catalysts for advanced bio-fuel production through catalytic biomass pyrolysis vapor upgrading: A review. *RSC Adv.* **2015**, *5*, 22234-22255.

(2) Bridgwater, A. V. Review of fast pyrolysis of biomass and product upgrading. *Biomass Bioenerg.* **2012**, *38*, 68-94.

(3) Galadima, A.; Muraza, O. In situ fast pyrolysis of biomass with zeolite catalysts for bioaromatics/gasoline production: A review. *Energ. Convers. Manage.* **2015**, *105*, 338-354.

(4) Huber, G. W.; Iborra, S.; Corma, A. Synthesis of transportation fuels from biomass: Chemistry, catalysts, and engineering. *Chem. Rev.* **2006**, *106*, 4044-4098.

(5) Kabir, G.; Hameed, B. H. Recent progress on catalytic pyrolysis of lignocellulosic biomass to high-grade bio-oil and bio-chemicals. *Renew. Sust. Energ. Rev.* **2017**, *70*, 945-967.

(6) Lappas, A. A.; Kalogiannis, K. G.; Iliopoulou, E. F.; Triantafyllidis, K. S.; Stefanidis, S. D. Catalytic pyrolysis of biomass for transportation fuels. *WIRES Energy Environ.* **2012**, *1*, 285-297.

(7) Liu, C.; Wang, H.; Karim, A. M.; Sun, J.; Wang, Y. Catalytic fast pyrolysis of lignocellulosic biomass. *Chem. Soc. Rev.* **2014**, *43*, 7594-7623.

(8) Tan, S.; Zhang, Z.; Sun, J.; Wang, Q. Recent progress of catalytic pyrolysis of biomass by HZSM-5. *Chinese J. Catal.* **2013**, *34*, 641-650.

(9) Venderbosch, R. H. A critical view on catalytic pyrolysis of biomass. *ChemSusChem* **2015**, *8*, 1306-1316.

(10) Won, W.; Maravelias, C. T. Thermal fractionation and catalytic upgrading of lignocellulosic biomass to biofuels: Process synthesis and analysis. *Renew. Energ.* **2017**, *114*, 357-366.

(11) Xu, M.; Mukarakate, C.; Robichaud, D. J.; Nimlos, M. R.; Richards, R. M.; Trewyn, B. G. Elucidating zeolite deactivation mechanisms during biomass catalytic fast pyrolysis from model reactions and zeolite syntheses. *Top. Catal.* **2016**, *59*, 73-85.

(12) Yang, H.; Yao, J.; Chen, G.; Ma, W.; Yan, B.; Qi, Y. Overview of upgrading of pyrolysis oil of biomass. *Enrgy. Proced.* **2014**, *61*, 1306-1309.

(13) Yildiz, G.; Ronsse, F.; Duren, R. V.; Prins, W. Challenges in the design and operation of processes for catalytic fast pyrolysis of woody biomass. *Renew. Sust. Energ. Rev.* **2016**, *57*, 1596-1610.

(14) Zhang, L.; Liu, R.; Yin, R.; Mei, Y. Upgrading of bio-oil from biomass fast pyrolysis in China: A review. *Renew. Sust. Energ. Rev.* **2013**, *24*, 66-72.

(15) Zhang, Q.; Chang, J.; Wang, T.; Xu, Y. Review of biomass pyrolysis oil properties and upgrading research. *Energ. Convers. Manage.* **2007**, *48*, 87-92.

(16) Bridgwater, A. V.; Meier, D.; Radlein, D. An overview of fast pyrolysis of biomass. *Org. Geochem.* **1999**, *30*, 1479-1493.

(17) Kan, T.; Strezov, V.; Evans, T. J. Lignocellulosic biomass pyrolysis: A review of product properties and effects of pyrolysis parameters. *Renew. Sust. Energ. Rev.* **2016**, *57*, 1126-1140.

(18) Mohan, D.; Pittman Jr, C. U.; Steele, P. H. Pyrolysis of wood/biomass for bio-oil: A critical review. *Energ. Fuel.* **2006**, *20*, 848-889.

(19) Czernik, S.; Bridgwater, A. V. Overview of applications of biomass fast pyrolysis oil. *Energ. Fuel.* **2004**, *18*, 590-598.

(20) Evans, R. J.; Milne, T. A. Molecular characterization of the pyrolysis of biomass. 1. Fundamentals. *Energ. Fuel.* **1987**, *1*, 123-137.

(21) Evans, R. J.; Milne, T. A. Molecular characterization of the pyrolysis of biomass. 2. Applications. *Energ. Fuel.* **1987**, *1*, 311-319.

(22) Mortensen, P. M.; Grunwaldt, J. D.; Jensen, P. A.; Knudsen, K. G.; Jensen, A. D. A review of catalytic upgrading of bio-oil to engine fuels. *Appl. Catal. A-Gen.* **2011**, *407*, 1-19.

(23) Carlson, T. R.; Tompsett, G. A.; Conner, W. C.; Huber, G. W. Aromatic production from catalytic fast pyrolysis of biomass-derived feedstocks. *Top. Catal.* **2009**, *52*, 241-252.

(24) To, A. T.; Resasco, D. E. Role of a phenolic pool in the conversion of m-cresol to aromatics over HY and HZSM-5 zeolites. *Appl. Catal. A-Gen.* **2014**, *487*, 62-71.

(25) Carlson, T. R.; Jae, J.; Huber, G. W. Mechanistic insights from isotopic studies of glucose conversion to aromatics over ZSM-5. *ChemCatChem* **2009**, *1*, 107-110.

(26) Mukarakate, C.; Zhang, X.; Stanton, A. R.; Robichaud, D. J.; Ciesielski, P. N.; Malhotra, K.; Donohoe, B. S.; Gjersing, E.; Evans, R. J.; Heroux, D. S.; Richards, R.; Iisa, K.; Nimlos, M. R. Real-time monitoring of the deactivation of HZSM-5 during upgrading of pine pyrolysis vapors. *Green Chem.* **2014**, *16*, 1444-1461.

(27) Du, S.; Gamliel, D. P.; Giotto, M. V.; Valla, J. A.; Bollas, G. M. Coke formation of model compounds relevant to pyrolysis bio-oil over ZSM-5. *Appl. Catal. A-Gen.* **2016**, *513*, 67-81.

(28) Fan, Y.; Cai, Y.; Li, X.; Yin, H.; Xia, J. Coking characteristics and deactivation mechanism of the HZSM-5 zeolite employed in the upgrading of biomass-derived vapors. *J. Ind. Eng. Chem.* **2017**, *46*, 139-149.

(29) Horne, P. A.; Williams, P. T. The effect of zeolite ZSM-5 catalyst deactivation during the upgrading of biomass-derived pyrolysis vapours. *J. Anal. Appl. Pyrol.* **1995**, *34*, 65-85.

(30) Li, Y.; Zhang, C.; Li, C.; Liu, Z.; Ge, W. Simulation of the effect of coke deposition on the diffusion of methane in zeolite ZSM-5. *Chem. Eng. J.* **2017**, *320*, 458-467.

(31) Shao, S.; Zhang, H.; Wang, Y.; Xiao, R.; Heng, L.; Shen, D. Catalytic pyrolysis of biomass-derived compounds: Coking kinetics and formation network. *Energ. Fuel.* **2015**, *29*, 1751-1757.

(32) Xu, M.; Mukarakate, C.; Iisa, K.; Budhi, S.; Menart, M.; Davidson, M.; Robichaud, D. J.; Nimlos, M. R.; Trewyn, B. G.; Richards, R. M. Deactivation of multilayered MFI nanosheet zeolite during upgrading of biomass pyrolysis vapors. *ACS Sustain. Chem. Eng.* **2017**, *5*, 5477-5484.

(33) Zhang, H.; Shao, S.; Xiao, R.; Shen, D.; Zeng, J. Characterization of coke deposition in the catalytic fast pyrolysis of biomass derivates. *Energ. Fuel.* **2014**, *28*, 52-57.

(34) Paasikallio, V.; Lindfors, C.; Kuoppala, E.; Solantausta, Y.; Oasmaa, A.; Lehto, J.; Lehtonen, J. Product quality and catalyst deactivation in a four day catalytic fast pyrolysis production run. *Green Chem.* **2014**, *16*, 3549-3559.

(35) Vitolo, S.; Bresci, B.; Seggiani, M.; Gallo, M. G. Catalytic upgrading of pyrolytic oils over HZSM-5 zeolite: Behaviour of the catalyst when used in repeated upgrading-regenerating cycles. *Fuel* **2001**, *80*, 17-26.

(36) Xian, X.; Ran, C.; Nai, C.; Yang, P.; Zhao, S.; Dong, L. Characterization of the location of coke deposited on spent HZSM-5 zeolite by special temperature-programmed oxidation and isothermal oxidation methods. *Appl. Catal. A-Gen.* **2017**, *547*, 37-51.

(37) Foust, T. D.; Ziegler, J. L.; Pannala, S.; Ciesielski, P.; Nimlos, M. R.; Robichaud, D. J. Predictive model for particle residence time distributions in riser reactors. Part 1: Model development and validation. *ACS Sustain. Chem. Eng.* **2017**, *5*, 2847-2856.

(38) Foust, T. D.; Ziegler, J. L.; Pannala, S.; Ciesielski, P.; Nimlos, M. R.; Robichaud, D. J. Catalyst residence time distributions in riser reactors for catalytic fast pyrolysis. Part 2:

Pilot-scale simulations and operational parameter study. *ACS Sustain. Chem. Eng.* **2017**, *5*, 2857-2866.

(39) Talmadge, M. S.; Baldwin, R. M.; Biddy, M. J.; McCormick, R. L.; Beckham, G. T.; Ferguson, G. A.; Czernik, S.; Magrini-Bair, K. A.; Foust, T. D.; Metelski, P. D.; Hetrick, C.; Nimlos, M. R. A perspective on oxygenated species in the refinery integration of pyrolysis oil. *Green Chem.* **2014**, *16*, 407-453.

(40) Mukarakate, C.; McBrayer, J. D.; Evans, T. J.; Budhi, S.; Robichaud, D. J.; Iisa, K.; Ten Dam, J.; Watson, M. J.; Baldwin, R. M.; Nimlos, M. R. Catalytic fast pyrolysis of biomass: The reactions of water and aromatic intermediates produces phenols. *Green Chem.* **2015**, *17*, 4217-4227.

(41) Iisa, K.; French, R. J.; Orton, K. A.; Budhi, S.; Mukarakate, C.; Stanton, A. R.; Yung, M. M.; Nimlos, M. R. Catalytic pyrolysis of pine over HZSM-5 with different binders. *Top. Catal.* **2016**, *59*, 94-108.

(42) Iisa, K.; French, R. J.; Orton, K. A.; Dutta, A.; Schaidle, J. A. Production of low-oxygen bio-oil via ex situ catalytic fast pyrolysis and hydrotreating. *Fuel* **2017**, *207*, 413-422.

(43) Iisa, K.; French, R. J.; Orton, K. A.; Yung, M. M.; Johnson, D. K.; Ten Dam, J.; Watson, M. J.; Nimlos, M. R. In Situ and ex situ catalytic pyrolysis of pine in a bench-scale fluidized bed reactor system. *Energ. Fuel.* **2016**, *30*, 2144-2157.

(44) Hu, C.; Xiao, R.; Zhang, H. Ex-situ catalytic fast pyrolysis of biomass over HZSM-5 in a two-stage fluidized-bed/fixed-bed combination reactor. *Bioresource Technol.* **2017**, *243*, 1133-1140.

(45) Wang, Y.; Wang, J. Multifaceted effects of HZSM-5 (Proton-exchanged Zeolite Socony Mobil-5) on catalytic cracking of pinewood pyrolysis vapor in a two-stage fixed bed reactor. *Bioresource Technol.* **2016**, *214*, 700-710.

(46) Dayton, D. C.; Carpenter, J. R.; Kataria, A.; Peters, J. E.; Barbee, D.; Mante, O. D.; Gupta, R. Design and operation of a pilot-scale catalytic biomass pyrolysis unit. *Green Chem.* **2015**, *17*, 4680-4689.

(47) Lappas, A. A.; Samolada, M. C.; Iatridis, D. K.; Voutetakis, S. S.; Vasalos, I. A. Biomass pyrolysis in a circulating fluid bed reactor for the production of fuels and chemicals. *Fuel* **2002**, *81*, 2087-2095.

(48) Paasikallio, V.; Kalogiannis, K.; Lappas, A.; Lehto, J.; Lehtonen, J. Catalytic fast pyrolysis: Influencing bio-oil quality with the catalyst-to-biomass ratio. *Energy Technol.* **2017**, *5*, 94-103.

(49) Iliopoulou, E. F.; Stefanidis, S.; Kalogiannis, K.; Psarras, A. C.; Delimitis, A.; Triantafyllidis, K. S.; Lappas, A. A. Pilot-scale validation of Co-ZSM-5 catalyst performance in the catalytic upgrading of biomass pyrolysis vapours. *Green Chem.* **2014**, *16*, 662-674.

(50) Boroson, M. L.; Howard, J. B.; Longwell, J. P.; Peters, W. A. Product yields and kinetics from the vapor phase cracking of wood pyrolysis tars. *AIChE J.* **1989**, *35*, 120-128.

(51) Solar, J.; de Marco, I.; Caballero, B. M.; Lopez-Urionabarrenechea, A.; Rodriguez, N.; Agirre, I.; Adrados, A. Influence of temperature and residence time in the pyrolysis of woody biomass waste in a continuous screw reactor. *Biomass Bioenerg.* **2016**, *95*, 416-423.

(52) Ledesma, E. B.; Hoang, J. N.; Nguyen, Q.; Hernandez, V.; Nguyen, M. P.; Batamo, S.; Fortune, C. K. Unimolecular decomposition pathway for the vapor-phase cracking of eugenol, a biomass tar compound. *Energ. Fuel.* **2013**, *27*, 6839-6846.

(53) Scott, D. S.; Piskorz, J.; Bergougnou, M. A.; Graham, R.; Overend, R. P. The role of temperature in the fast pyrolysis of cellulose and wood. *Ind Eng. Chem. Res.* **1988**, *27*, 8-15.

(54) Uddin, M. N.; Daud, W. M. A. W.; Abbas, H. F. Effects of pyrolysis parameters on hydrogen formations from biomass: a review. *RSC Adv.* **2014**, *4*, 10467-10490.

(55) French, R.; Czernik, S. Catalytic pyrolysis of biomass for biofuels production. *Fuel Process. Technol.* **2010**, *91*, 25-32.

(56) Williams, P. T.; Nugranad, N. Comparison of products from the pyrolysis and catalytic pyrolysis of rice husks. *Energy* **2000**, *25*, 493-513.

(57) Hoff, T. C.; Holmes, M. J.; Proano-Aviles, J.; Emdadi, L.; Liu, D.; Brown, R. C.; Tessonnier, J. P. Decoupling the role of external mass transfer and intracrystalline pore diffusion on the selectivity of HZSM-5 for the catalytic fast pyrolysis of biomass. *ACS Sustain. Chem. Eng.* **2017**, *5*, 8766-8776.

(58) Thompson, L. C.; Ciesielski, P. N.; Jarvis, M. W.; Mukarakate, C.; Nimlos, M. R.; Donohoe, B. S. Estimating the temperature experienced by biomass particles during fast pyrolysis using microscopic analysis of biochars. *Energ. Fuel.* **2017**, *31*, 8193-8201.

(59) Agblevor, F. A.; Beis, S.; Mante, O.; Abdoulmoumine, N. Fractional catalytic pyrolysis of hybrid poplar wood. *Ind. Eng. Chem. Res.* **2010**, *49*, 3533-3538.

(60) Stefanidis, S. D.; Kalogiannis, K. G.; Iliopoulou, E. F.; Lappas, A. A.; Pilavachi, P. A. In-situ upgrading of biomass pyrolysis vapors: Catalyst screening on a fixed bed reactor. *Bioresource Technol.* **2011**, *102*, 8261-8267.

(61) Hammer, N. L.; Garrido, R. A.; Starcevich, J.; Coe, C. G.; Satrio, J. A. Two-step pyrolysis process for producing high quality bio-oils. *Ind Eng. Chem. Res.* **2015**, *54*, 10629-10637.

(62) Bird, R. B.; Stewart, W. E.; Lightfoot, E. N. *Transport phenomena*; 2nd rev ed.; Wiley: New York, 2007.

(63) Iliopoulou, E. F.; Stefanidis, S. D.; Kalogiannis, K. G.; Delimitis, A.; Lappas, A. A.; Triantafyllidis, K. S. Catalytic upgrading of biomass pyrolysis vapors using transition metal-modified ZSM-5 zeolite. *Appl. Catal. B-Environ.* **2012**, *127*, 281-290.

TOC/Abstract Graphic: For Table of Contents Use Only

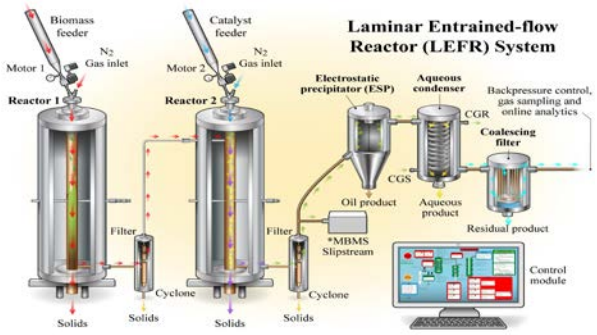

Synopsis

Catalytic fast-pyrolysis of biomass via a bench-scale continuous-flow reactor platform offers a sustainable approach for CFP optimization and catalyst screening utilizable in process scale-up.